Original Article

Journal of Tissue Engineering
Volume 6: 1–10

DOI: 10.1177/2041731415611717
tej.sagepub.com
SAGE

AAV vector encoding human $VEGF_{165}$–transduced pectineus muscular flaps increase the formation of new tissue through induction of angiogenesis in an in vivo chamber for tissue engineering: A technique to enhance tissue and vessels in microsurgically engineered tissue

Silvia Moimas[1,2], Benedetto Manasseri[3], Giuseppe Cuccia[4], Francesco Stagno d'Alcontres[5], Stefano Geuna[6], Lucia Pattarini[7], Lorena Zentilin[1], Mauro Giacca[1,2] and Michele R Colonna[5]

Abstract

In regenerative medicine, new approaches are required for the creation of tissue substitutes, and the interplay between different research areas, such as tissue engineering, microsurgery and gene therapy, is mandatory. In this article, we report a modification of a published model of tissue engineering, based on an arterio-venous loop enveloped in a cross-linked collagen–glycosaminoglycan template, which acts as an isolated chamber for angiogenesis and new tissue formation. In order to foster tissue formation within the chamber, which entails on the development of new vessels, we wondered whether we might combine tissue engineering with a gene therapy approach. Based on the well-described tropism of adeno-associated viral vectors for post-mitotic tissues, a muscular flap was harvested from the pectineus muscle, inserted into the chamber and transduced by either AAV vector encoding human $VEGF_{165}$ or AAV vector expressing the reporter gene β-galactosidase, as a control. Histological analysis of the specimens showed that muscle transduction by AAV vector encoding human $VEGF_{165}$ resulted in enhanced tissue formation, with a significant increase in the number of arterioles within the chamber in comparison with the previously published model. Pectineus muscular flap, transduced by adeno-associated viral vectors, acted as a source of the proangiogenic factor vascular endothelial growth factor, thus inducing a consistent enhancement of vessel growth into the newly formed tissue within the chamber. In conclusion, our present findings combine three different research fields such as microsurgery, tissue engineering and gene therapy, suggesting and showing the feasibility of a mixed approach for regenerative medicine.

Keywords

Arterio-venous loop, collagen/glycosaminoglycan matrix, angiogenesis, gene therapy, tissue engineering, microsurgery

Received: 28 May 2015; accepted: 8 September 2015

[1]Molecular Medicine Laboratory, International Centre for Genetic Engineering and Biotechnology (ICGEB), Trieste, Italy
[2]Department of Medical Sciences, Faculty of Medicine, University of Trieste, Trieste, Italy
[3]Plastic Surgery Unit, Niguarda Ca' Granda Hospital, Milan, Italy
[4]Plastic Surgery, Villa Sofia – Cervello General Hospital, Palermo, Italy
[5]Department of Clinical and Experimental Medical and Surgical Specialties and Odontostomatology, University of Messina, Messina, Italy
[6]Department of Clinical and Biological Sciences, University of Turin Medical School, Turin, Italy
[7]Immunité et Cancer, Institut Curie, Paris, France

Corresponding author:
Michele R Colonna, Department of Clinical and Experimental Medical and Surgical Specialties and Odontostomatology, University of Messina, Viale della Libertà 395/Y, 98121 Messina, Italy.
Email: mrcolonna1@gmail.com

Introduction

Since the rise of tissue engineering, the development of biological substitutes in medical research has been a key issue in order to develop new strategies to replace lost or damaged tissues. The research field focused on new tissue formation is improving day by day, and it is nowadays facing the problem of poor tissue vascularization.[1–4] The angiogenic process, which takes place within the scaffolds, is adequate to allow cellular oxygen supply, whereas it might not be sufficient to sustain tissue survival. Thus, in order to improve tissue vascularization, several approaches are currently under investigations, such as the addition of angiogenic factors, the seeding of cells engineered for the production of growth factors within the scaffold or the development of microsurgical strategies.

Focusing on the usage of factors, several attempts have already been developed by the use of one or more recombinant proteins either alone or in combination such as vascular endothelial growth factor (VEGF), basic fibroblast growth factor (bFGF) or platelet-derived growth factor b (PDGF-b) leading to promising results that were shown to be affected by the short half-life of the recombinant factors.[5] Therefore, studies aimed to control the protein release from the scaffold, for instance by the application of slow release devices or modified matrix, were developed and led to better results suggesting that these approaches might be feasible.[6–10] Moreover, concerning the microsurgical techniques, a promising approach has been developed by Morrison, who has combined tissue engineering and microsurgery.[11–13] Focusing on the development of innovative approaches to enhance the formation of new blood vessel and, most importantly, the generation of a vascularized new tissue within a scaffold, a novel promising method has been described, based on a microsurgical arterio-venous loop (AVL) embedded in a collagen-based matrix.[14] In this model, the main driver for blood vessel formation has been identified in the shear stress within the vessels of the AVL.[4]

A research area that is nowadays opening a new scenario in the tissue engineering field is gene therapy, which might be combined with the previously described approaches to improve them and to overcome their limitations. The use of recombinant vectors for the production of secreted proteins is widely used in research,[15–17] and clinical trials have already been performed, such as for the treatment of haemophilia.[18,19] Among the different viral vectors that have been used so far, recombinant adeno-associated viral (rAAV) ones are emerging as feasible candidates for gene therapy due to their appealing features. Of interest, they are able to transduce post-mitotic cells and are characterized by a high tropism for skeletal muscle. Moreover, rAAVs can persist in the transduced cells, leading to long-lasting protein expression. We herein suggest a modification of the novel microsurgically induced regeneration chamber with the insertion of a muscle flap, which can be transduced by rAAVs leading to the secretion of VEGF that eventually will induce an enhancement of the already documented creation of newly formed fibrovascular tissue inside the chamber.

Hence, we propose an approach that combines adeno-associated viral (AAV)-based gene therapy, a collagen scaffold, the pectineus muscular flap and a microsurgical AVL. The pectineus muscular flap is, in the proposed model, inserted into the tissue chamber, presenting also the AVL, and injected with AAV vector encoding human $VEGF_{165}$ (AAV-$VEGF_{165}$) in order to induce the production of VEGF inside the chamber that might improve the angiogenic process and might eventually foster the growth of the implant.

Material and methods

Animals

In all, 21 adult male Wistar rats, weighting 300–350 g, were used for this study. All procedures were carried out under general anaesthesia using Zoletil (Virbac, Carros, France) 40 mg/kg in combination with xylazine (Sigma Aldrich, St. Louis, MO, USA) 15 mg/kg intramuscularly (i.m.). During surgery and for the following 10 days, rats were treated with heparin in order to avoid the formation of thrombi within the AVL forming vessels. The animals were housed in single cages and fed ad libitum.

Animal care and treatment were conducted in conformity with institutional guidelines in compliance with national and international laws and policies (EEC Council Directive 86/609, OJL 358, 12 December 1987) after institutional review board approval.

Generation of the collagen chamber

A previously described AVL model was modified:[14] a vein graft was harvested from one groin and used as a microvascular loop between the femoral artery and vein in the contralateral leg. End-to-side anastomoses were performed with 11/0 nylon sutures on both recipient artery and vein. Then, the vein graft was harvested as long as possible (about 2.4 cm) to enhance angiogenesis from the loop; the previously described chamber was closed folding the template on itself and suturing its free margins together. As the template is enveloped by a silicone layer, the outer envelope of the chamber is silicone; this model of the chamber encloses the AVL and has been demonstrated as a valid system for fostering neovascularization as well as new loose connective tissue formation. In order to test whether we were able to improve the formation of new tissue within the collagen chamber, we added an element to this model, represented by a muscle flap. Skeletal muscle has already been shown to be efficiently transduced by rAAVs. In order to preserve muscle integrity, we conceived a model of local muscle flap (pedicled), and

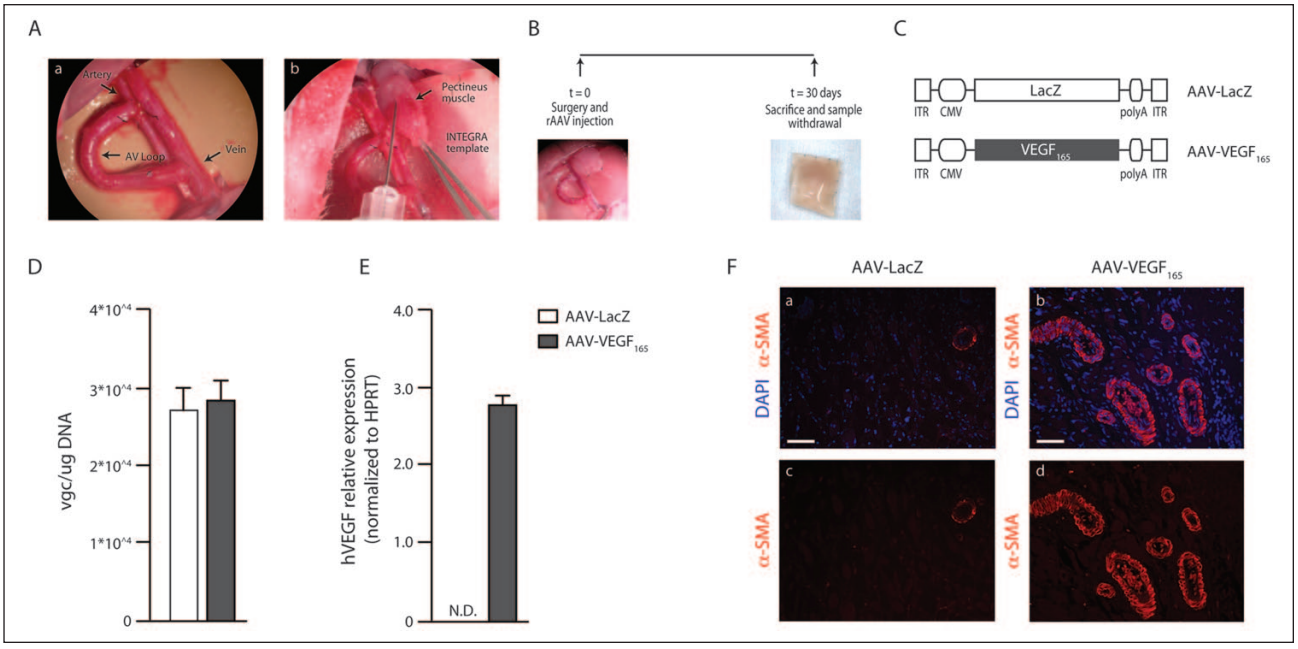

Figure 1. Creation of a tissue chamber, based on an arterio-venous loop (AVL), feasible for gene therapy. (A) Tissue chamber was created (inset a) and a pectineus muscular flap was inserted into the chamber. The muscle was injected with either AAV-LacZ or AAV-$VEGF_{165}$ before closure of the chamber (inset b). (B) Schematic representation of the experimental flow chart. (C) Schematic representation of rAAVs used in the study (ITR: inverted terminal repeats). (D) Samples were harvested 30 days after surgery, DNA extracted and viral load quantified by real-time PCR (vgc: viral genome copies). Data are expressed as mean ± SEM. (E) Samples were harvested 30 days after surgery, RNA extracted and cDNA synthesized. Expression of the transgene was quantified by real-time PCR; hVEGF expression was not detectable (ND) in the control sample. Data are expressed as mean ± SEM. (F) Representative images of the tissue chamber sample stained for α-SMA (red); nuclei are counterstained with DAPI (blue) (insets a and b: AAV-LacZ and AAV-$VEGF_{165}$, respectively). Several α-SMA-positive vessels can be observed in the AAV-$VEGF_{165}$ sample, suggesting the effect of $VEGF_{165}$ overexpression. Split α-SMA images from AAV-LacZ and AAV-$VEGF_{165}$ samples are reported in insets c and d, respectively. Vessels are interspersed within the muscle fibres that can be identified as background signal. Scale bar = 50 μm.

due to the anatomical location, we chose the pectineus muscle as the target tissue to be inserted into the chamber for rAAV transduction. The pectineus flap, comprising its proximal part and sizing mostly 1 cm, was elevated and left pedicled under microscope magnification. One or two delicate stitches were tied to fix the muscle to the collagen matrix and to avoid residual contraction. The dermal template (INTEGRA™) was then folded on itself, maintaining the outer silicon layer, and secured by some suture stitches as a sandwich including the loop and the muscular flap (Figure 1(A)).

Adult male Wistar rats were divided into three groups ($n = 7$ per group) according to the treatment (no muscle, AAV vector expressing the reporter gene β-galactosidase (AAV-LacZ) and AAV-$VEGF_{165}$); the tissue chamber was created as previously described and the isolated muscular flap was injected with 50 μL of either a control AAV-LacZ or the human $VEGF_{165}$ isoform (AAV-$VEGF_{165}$) (Figure 1(A)), and the chamber was then closed. The first group acted as control. After 30 days, dermal implants were excised and analysed to detect the formation of new tissue and the presence of vessels. A schematic representation of the experimental flow chart is reported in Figure 1(B).

Recombinant AAV vectors

The rAAV vectors used in this study were produced by the AAV Vector Unit (AVU) at ICGEB Trieste (http://www.icgeb.org/avu-core-facility.html), according to the established procedures.[20–22] AAV2 vectors are used in this study, due to serotype tropism for skeletal muscles, and they express either $VEGF_{165}$ or β-galactosidase complementary DNA (cDNA) under the control of the constitutive cytomegalovirus (CMV) immediate early promoter. All the viral stocks used had a titre $\geq 1 \times 10^{12}$ viral genome particles/mL. A schematic representation of rAAVs is reported in Figure 1(C).

Histochemistry, immunofluorescence and morphometric analysis

On day 30, tissue chambers were harvested, following the previously described techniques.[14] Briefly, rats were anaesthetized, the chambers were exposed, vessels were ligated proximally and distally and the specimens were harvested and immediately fixed in 10% formalin and embedded in paraffin. The 5-μm histological sections were stained with Azan trichrome staining (BioOptica, Milan, Italy) or

Table 1. Assays used for real-time PCR.

Target	Assay type	Real-time probe	Assay code or primer/probe sequences
hVEGF	Pre-developed	FAM	Hs00173626_m1
HPRT	Pre-developed	VIC	Rn01527840_m1
CMV	Custom	FAM	Primer Fw 5′-TGGGCGGTAGGCGTGTA-3′ Primer Rv 5′-GATCTGACGGTTCACTAAACGAG-3′ Probe 5′-CCTGGAGACGCCATC-3′

PCR: polymerase chain reaction; hVEGF: human vascular endothelial growth factor; CMV: cytomegalovirus; HPRT: hypoxanthine guanine phosphoribosyltransferase.
All assays are from Life Technologies.

processed for immunofluorescence. The following primary antibodies were used: Cy3-coniugated anti–alpha smooth muscle actin (α-SMA) primary antibody (clone 1A4; Sigma) diluted 1:200 in blocking buffer was used to label smooth muscle cells/pericytes and myofibroblats. Anti-vimentin (sc-6260; Santa Cruz Biotechnology, Dallas, USA) diluted 1:50 in blocking buffer was used to label fibroblasts, and heat-induced antigen retrieval at pH 6 was performed; AlexaFluor 594 anti-mouse antibody (Molecular Probes, Thermo Fisher Scientific, Whaltman, MA USA) diluted 1:500 in blocking buffer was used as secondary antibody. Fluorescein-labelled *Lycopersicon esculentum* Lectin (FL-1171; Vector Laboratories, Burlingame, CA, USA) diluted 1:100 in blocking buffer was used to label endothelial cells. 4′,6-diamidino-2-phenylindole (DAPI) (Vectashield, Vector Laboratories, Burlingame, CA, USA) fluorescent staining was used to recognize cell nuclei. Images were acquired at room temperature with a DMLB upright fluorescence microscope (Leica Microsystems, Wetzlar, Germany) equipped with a charge-coupled device camera (CoolSNAP CF; Roper Scientific, Trenton, NJ, USA) using MetaView 4.6 quantitative analysis software (MDS Analytical Technologies, Toronto, Canada). Images from Azan trichrome–stained sections were acquired by Leica Laser Microdissector LMD7000 (Leica Microsystems) equipped with a three charge-coupled device colour Hitachi HV-C20A camera (Hitachi, Tokyo, Japan) using Leica IM 1000 software (Leica Microsystems). For the quantification of the tissue within the chamber, the whole area occupied by the stained tissue was quantified by the use of ImageJ software. For the quantification of vessel number, at least 10 fields for each section were analysed. Relative areas occupied by differently stained cells were quantified by the use of ImageJ software.

DNA extraction and AAV detection within the tissue chamber

DNA was extracted from paraffin-embedded specimens, and five sections (50 µm) were deparaffinized, hydrated and digested with proteinase K. DNA content was quantified by means of the Qubit fluorometer (Invitrogen); 50 ng was subsequently used for AAV quantification performed by real-time polymerase chain reaction (PCR), using pre-developed and custom-designed assays (Applied Biosystems, Thermo Fisher Scientific, Whaltman, MA, USA). Values are expressed as the number of viral genome copies (vgc) per microgram genomic DNA using an external calibration curve. A list of the assays used is reported in Table 1. Amplifications were carried out in a CFX96 Real-Time PCR Detection System (Bio-Rad Laboratories, Hercules, CA USA).

RNA isolation and transgene expression analysis

RNA was extracted from frozen samples using TriZol reagent (Life Technologies, Thermo Fisher Scientific, Whaltman, MA, USA) and reversed transcribed using hexamerix random primers (Life Technologies, Thermo Fisher Scientific, Whaltman, MA, USA). The cDNA was subsequently used for transgene expression analysis performed by real-time PCR; the housekeeping gene hypoxanthine guanine phosphoribosyltransferase (HPRT) was used to normalize the results. A list of the assays used is reported in Table 1. Amplifications were carried out in a CFX96 Real-Time PCR Detection System (Bio-Rad).

Statistics

Data are presented as mean ± standard error of the mean (SEM). Pair-wise comparison between groups was performed using the Student's *t*-test, whereas one-way analysis of variance (ANOVA) and Bonferroni post hoc tests were used to compare multiple groups. A value of $p < 0.05$ was considered statistically significant.

Results

Description of the model and detection of AAV within the tissue chamber

We herein propose a modification of a previously described AVL model by means of a gene therapy approach. In order to create an AVL, a vein graft was harvested from one groin

and used as a microvascular loop between the femoral artery and vein in the contralateral leg. End-to-side anastomoses were performed with 11/0 nylon sutures on both recipient artery and vein. The AVL was created on a collagen-based template, and a muscular flap from the pectineus muscle was inserted in close proximity and transduced by rAAVs. The muscle was chosen as a target tissue due to the high tropism of rAAV, serotype 2, for the skeletal muscle. The described chamber was then closed folding the template on itself and suturing its free margins together. In order to confirm the presence of the injected vectors within the chamber, we analysed DNA extracted from the samples isolated 30 days after surgery and quantified the viral load by means of real-time PCR, as described in section 'Material and methods'. In all the samples, we were able to detect the presence of rAAV genomes, as reported in Figure 1(D). Moreover, we analysed the expression of the transgene, and we could detect the expression of human VEGF in the AAV-$VEGF_{165}$ samples as reported in Figure 1(E).

AAV-$VEGF_{165}$ angiogenic effect within the tissue chamber

The transgene expression analysis confirmed the expression of human VEGF in the pectineus muscle within the chamber. Therefore, to assess the functional effect of rAAV transduction, a histological analysis was performed on the muscular flap in order to check for the angiogenic response induced by $VEGF_{165}$ overexpression. As previously reported by our group, $VEGF_{165}$ is able to induce the formation of small arterioles that can be visualized by an immunofluorescence staining for α-SMA.[16,20,23] Interestingly, the muscular tissue was preserved intact inside the collagen implant and the angiogenic effect of $VEGF_{165}$ could be confirmed by the presence of α-SMA-positive vessels surrounding the muscle fibres; AAV-LacZ-injected samples were used as controls (Figure 1(F)).

Induction of new tissue formation

The detection of the rAAV DNA within the chamber and the angiogenic effect observed in the muscular flap suggested the feasibility of our combined tissue engineering–gene therapy approach. Thereby, in order to assess whether the expression of $VEGF_{165}$ by the transduced muscle fibres might improve the formation of new tissue within the chamber, we performed an Azan trichrome staining and quantified the newly formed tissue by means of ImageJ software.

The samples were harvested at 1 month, time not sufficient for complete matrix collagen degradation; indeed, trabeculae were still detectable in all the samples, filling almost 20% of the section area. Due to the presence of the original collagen matrix, we were not able to quantify solely the newly formed tissue; instead we quantified the whole area occupied by the original matrix and the newly deposited tissue. Our quantification confirmed the data reported in the first described AVL model; indeed, in the samples with no muscle flap, the tissue filled 65% of the area, whereas in the AAV-LacZ group it raised up to 72% and in the AAV-$VEGF_{165}$ group it reached 80% of the section area ($p<0.05$ AAV-LacZ vs control; $p<0.001$ AAV-$VEGF_{165}$ vs control; $p<0.01$ AAV-$VEGF_{165}$ vs AAV-LacZ). Representative images and quantification are reported in Figure 2. Surprisingly, the muscle flap injected with AAV-LacZ was also able to exert an effect on the chamber environment, leading to an increase in tissue formation but not at the same extent as observed upon transduction with AAV-$VEGF_{165}$. A further histological analysis of the samples allowed us to obtain an accurate characterization of the newly formed tissue. The quantification of the number of cells present within the chamber, performed by quantifying the relative area occupied by DAPI nuclear staining, showed an increase in both the AAV-treated groups compared to the control one (7.84%±0.63% for control, 10.72%±0.52% for AAV-LacZ and 13.81%±0.55% for AAV-$VEGF_{165}$; $p<0.001$ AAV-$VEGF_{165}$ vs control; $p<0.05$ AAV-$VEGF_{165}$ vs AAV-LacZ). Representative images and quantification are reported in Supplementary Figure 1.

These results suggest that the presence of the muscle flap might contribute to new tissue formation by secreting growth factors. Moreover, muscle transduction by AAV-$VEGF_{165}$ is able to further enhance it.

Vessel formation is improved by $VEGF_{165}$ overexpression

The Azan trichrome staining also allowed us to detect a consistent number of new vessels interspersed within the collagen trabeculae of the artificial tissue (Figure 2(A)). To assess whether new tissue formation might be associated or even favoured by an increased blood supply, as already showed in previous AVL models,[14] we analysed the presence of α-SMA-positive vessels by immunofluorescence staining, which showed that many new small arterioles were indeed contributing to the perfusion of the tissue chamber (Figure 3(A)). A quantitative analysis revealed a pronounced increase in the number of vessels present within the chamber: 2.22±0.24 vessels per section were detected in the control group, while 4.93±0.42 and 8.27±0.50 vessels per section were detected in AAV-LacZ- and AAV-$VEGF_{165}$-treated animals, respectively ($p<0.05$ AAV-LacZ vs control; $p<0.05$ AAV-$VEGF_{165}$ vs control; $p<0.05$ AAV-$VEGF_{165}$ vs AAV-LacZ) (Figure 3(B)).

Although not observed in all samples at the same extent, the angiogenic effect in some sections was impressive, especially in close proximity to the vein graft. As reported in Figure 3(C), the analysis of serial sections revealed that more than 10 vessels per section were detected only in the AAV-$VEGF_{165}$ group, whereas in the AAV-LacZ group

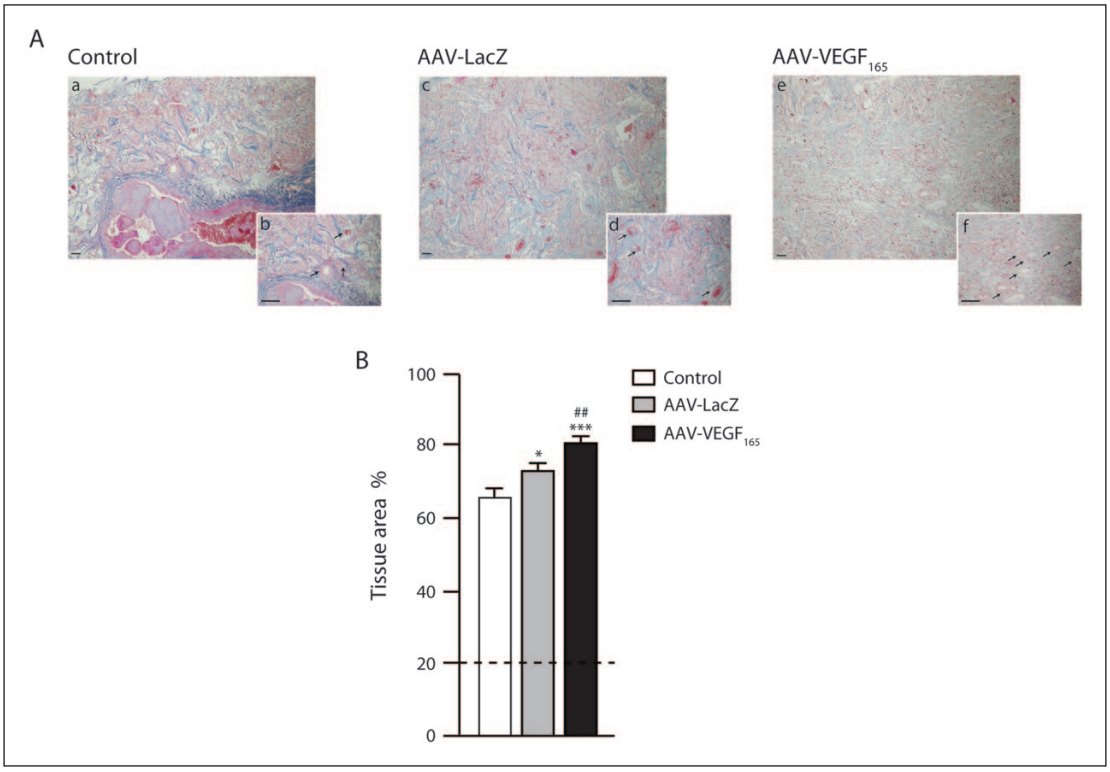

Figure 2. The presence of a muscular flap within the chamber enhances the formation of new tissue. (A) Azan trichrome staining of tissue chambers from control (insets a and b), AAV-LacZ-treated animals (insets c and d) and AAV-$VEGF_{165}$-treated animals (insets e and f). The staining showed the formation of tissue within the chamber. The presence of the muscular flap was able to increase tissue formation (insets c and d), and it was further increased upon $VEGF_{165}$ overexpression (insets e and f). Vessels can be identified and are shown by arrows (insets b, c and d). Scale bar = 100 µm. (B) Quantification of the area occupied by tissue; it is expressed as percentage of the total area. The samples were withdrawn 30 days after surgery, time not sufficient for collagen trabeculae degradation; thus, they were still detectable and occupied about 20% of the total area, as reported in the plot by the dashed line. Data are expressed as mean ± SEM. *$p < 0.05$, ***$p < 0.001$ versus control; ##$p < 0.05$ versus AAV-LacZ group.

vessels were always fewer. Interestingly, in some of the AAV-$VEGF_{165}$ sample sections, we observed the presence of few enlarged vessels, with a thin α-SMA cell layer and characterized by an irregular shape, resembling vascular lacunae, previously described by our group[16,23] (Figure 4).

To confirm that the α-SMA-positive structures were indeed vessels, a lectin staining was performed for the identification of endothelial cells. As shown in Supplementary Figure 2, an inner layer of endothelial cells can be observed in close proximity to the α-SMA-positive structures and the vessel lumen can be recognized. Interestingly, the lectin staining highlighted the presence of endothelial cells not surrounded by α-SMA-positive cells, thus suggesting the presence of capillaries. Therefore, we performed a further histological analysis on the tissue sections for the identification of the different components of the newly formed tissue. Besides the presence of arterioles revealed by the α-SMA staining (Figure 5(A)), we were able to detect several lectin-positive vessels suggesting a strong angiogenic process (Figure 5(B)). The newly formed vascular network was interspersed within the newly deposited collagen matrix and several cell nuclei were detected, as reported in Figure 2 and 3. Thereby, we wondered whether fibroblasts were a cellular population composing the new tissue. Thus, a vimentin staining was performed and highlighted a massive presence of fibroblasts suggesting an important role in tissue formation (Figure 5(C)).

Discussion

In medicine, the research of alternative sources for tissue substitutes and innovative approaches to enhance tissue regeneration is a major challenge. Tissue engineering has largely spread out in this respect, and one of the key issues that is emerging nowadays is the demand for vascularization of the new templates in order to improve cell and tissue survival.

Several approaches aimed to enhance the formation of new vascularized tissue have been described so far, and recently, Morrison and colleagues showed that a microsurgical AVL-based method could lead to the formation of a highly vascularized tissue within a biological scaffold. Indeed, these authors reported that the insertion of an AVL

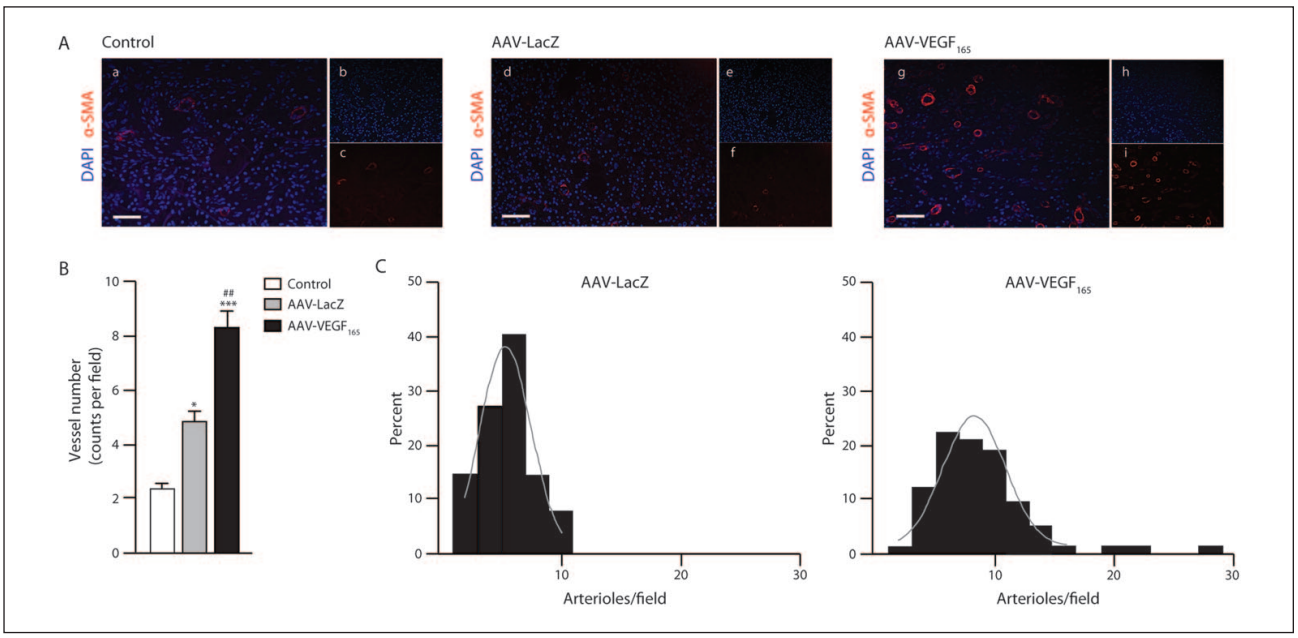

Figure 3. Tissue formation, sustained by $VEGF_{165}$ overexpression, entails on the induction of a strong angiogenic response. (A) Representative images from control, AAV-LacZ and AAV-$VEGF_{165}$ samples. Sections were stained for α-SMA (red) and nuclei were counterstained with DAPI (blue) (insets a, d and g). Split α-SMA and DAPI signals are shown in the small panels b, c, e, f, h and i on the right side of the respective merged pictures. Scale bar = 50 µm. (B) Quantitative evaluation of the vascular parameter α-SMA-positive vessel number. Data are expressed as mean ± SEM. *$p < 0.05$, ***$p < 0.001$ versus control; ##$p < 0.01$ versus AAV-LacZ group. (C) The angiogenic response was also analysed taking into account the distribution of vessels per section. The histograms show the distribution of vessels per section, with a normal distribution curve superimposed. The distribution, in the AAV-$VEGF_{165}$ group (right side), skewed towards the right compared to the AAV-LacZ group (left side) and also included a significant number of sections with more than 10 vessels.

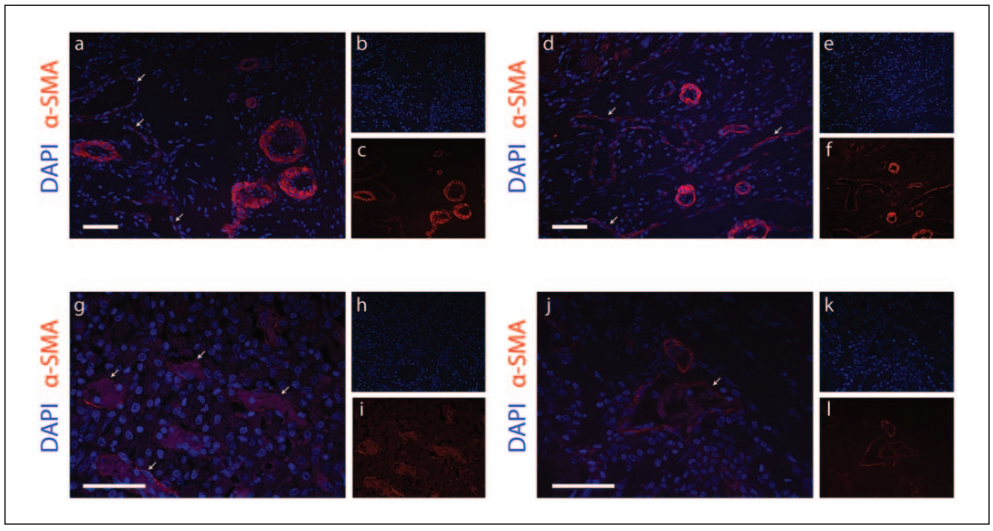

Figure 4. $VEGF_{165}$ overexpression induces the formation of enlarged vessels. Images from AAV-$VEGF_{165}$ samples. Sections were stained for α-SMA (red) and nuclei were counterstained with DAPI (blue) (insets a, d, g and j). Split α-SMA and DAPI signals are shown in the small panels b, c, e, f, h, i, k and l on the right side of the respective merged pictures. Enlarged vessels characterized by a thin layer of α-SMA-positive cells are shown by arrows. The presence of erythrocytes inside the vessels can be appreciated from higher magnification images (insets g and j). Scale bar = 50 µm.

into a fibrin-rich tissue chamber enhances the formation of a vascularized soft tissue that resembles a connective tissue.[13]

More recently, a novel microsurgical model has been described, based on the usage of a commercially available cross-linked collagen/glycosaminoglycan (GAG) template

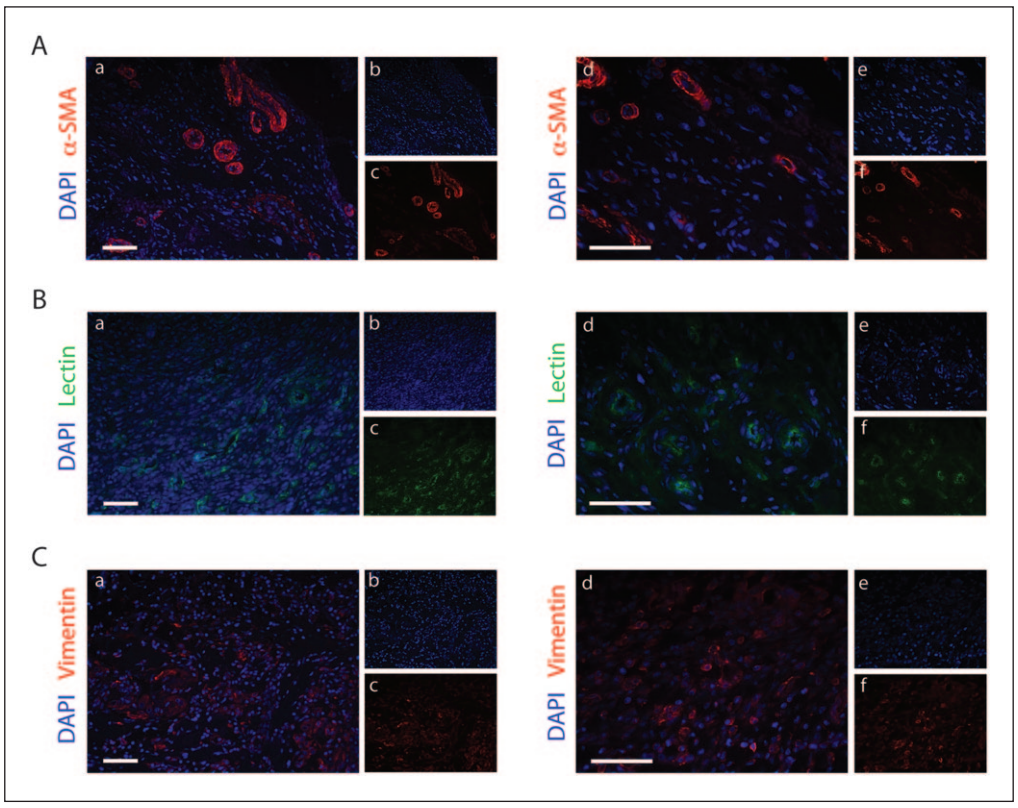

Figure 5. Characterization of the cellular populations within the newly formed tissue. (A) Representative images from AAV-$VEGF_{165}$ samples. Sections were stained for α-SMA (red) and nuclei were counterstained with DAPI (blue) (insets a and d). Split α-SMA and DAPI signals are shown in the small panels b, c, d and e on the right side of the respective merged pictures. Higher magnification images are reported in insets d, e and f. Scale bar = 50 µm. (B) Representative images from AAV-$VEGF_{165}$ samples. Sections were stained by lectin (green) and nuclei were counterstained with DAPI (blue) (insets a and d). Split lectin and DAPI signals are shown in the small panels b, c, d and e on the right side of the respective merged pictures. Higher magnification images are reported in insets d, e and f. Scale bar = 50 µm. (C) Representative images from AAV-$VEGF_{165}$ samples. Sections were stained for vimentin (red) and nuclei were counterstained with DAPI (blue) (insets a and d). Split vimentin and DAPI signals are shown in the small panels b, c, d and e on the right side of the respective merged pictures. Higher magnification images are reported in insets d, e and f. Scale bar = 50 µm.

as a new type of matrix to envelop an AVL in the rat groin.[14] Of interest, in this model the process of angiogenesis has been deeply characterized, and tensional and shear stress forces were shown to be the key factors for the angiogenic stimuli.[4]

In order to improve this previous model and to foster vessel formation by the expression of angiogenic factors, such as VEGF, we took advantage of the gene transfer technology based on rAAV vectors. Indeed, a muscle pedicle, which is a suitable candidate for rAAV transduction,[24,25] was inserted inside the collagen/GAG scaffold. For this purpose, in our new surgical model, we chose the pectineus muscle, which is close to both the loop and the chamber, in the rat groin. In addition, it was also selected due to its vascular and anatomical features. Thus, the muscular flap was inserted in the collagen/GAG implant, still connected to the circulation by a vascular pedicle that ensures tissue perfusion and long-term survival, features needed for transgene expression by the muscle fibres. At 1 month after surgery, we were able to recover collagen/GAG implants in which the muscle flap tissue was still intact and connected to the vasculature. Furthermore, the presence of rAAV genomes and the expression of the transgene could be detected; we also observed a strong angiogenic response in the muscle, as previously reported in other models.[16,21,23,26]

To better characterize our collagen chamber, we analysed the newly formed tissue and we observed a slight improvement in the tissue area in the presence of the muscle flap injected with a control vector, which was even increased upon $VEGF_{165}$ expression. Surprisingly, an increase in the new tissue area was also detected in the AAV-LacZ samples, and this effect might be due to the expression of proangiogenic factors, such as VEGF, in response to hypoxia by the muscular flap within the chamber.[27–29] Moreover, we observed that the extension of the area occupied by the new tissue correlated with the formation of α-SMA-positive vessels within the chamber. Indeed, newly formed vessels were detected in both LacZ and

$VEGF_{165}$ expressing chambers, with a stronger effect in the $VEGF_{165}$-treated animals, confirming the notion that, also in this model, VEGF exerts an angiogenic effect. A more detailed analysis on the vasculature showed that in the presence of VEGF the number of arterioles per section was increased, supporting and enhancing the finding that VEGF is an angiogenic factor, and in agreement with data previously reported in other mouse models.[16,23] A characterization of the cellular populations composing the new tissue revealed the presence of endothelial cells suggesting an ongoing angiogenic process and the massive presence of fibroblasts which might be involved in matrix deposition.

Additionally, we reported the presence of some enlarged vessels, resembling the vascular lacunae observed previously in the VEGF-treated muscles,[16,23] suggesting that the process of angiogenesis is mainly driven by VEGF in the described model.

Of notice, a strong angiogenic effect was observed not only in close proximity to the transduced muscle, likely sustained by the secreted factor, thus suggesting that the muscular flap might act as a bioreactor for secreted factors upon rAAV transduction.

Conclusion

The results obtained in this animal model confirmed the feasible use of AAV-$VEGF_{165}$ as a tool to enhance the formation of new tissue within an in vivo chamber for tissue engineering. Moreover, the increased number of α-SMA-positive vessels in the VEGF-treated animals suggested that the formation of new tissue might entail on the angiogenic process.

Our regeneration chamber looks as a promising tool in tissue engineering, particularly as it acts as an isolated chamber, which does not allow interference from the surrounding tissues. The creation of a highly vascularized tissue chamber which can be microsurgically transferred to another site, due to the presence of a vascular pedicle, might be appealing for reconstructive surgery.

As a future perspective, our chamber might be envisioned as a bioreactor and might be viewed as a tissue chamber for the in vivo expansion and differentiation of cells potentially enriched in precursor or stem cells.

Acknowledgements

S.M., B.M. and G.C. contributed equally to this work.

Declaration of conflicting interests

The author(s) declared no potential conflicts of interest with respect to the research, authorship and/or publication of this article.

Funding

The author(s) disclosed receipt of the following financial support for the research, authorship, and/or publication of this article: The Authors received funding for the research and publication from SIAD Healthcare Spa, Italy.

References

1. Polykandriotis E, Arkudas A, Horch RE, et al. Autonomously vascularized cellular constructs in tissue engineering: opening a new perspective for biomedical science. *J Cell Mol Med* 2007; 11(1): 6–20.
2. Nomi M, Atala A, Coppi PD, et al. Principals of neovascularization for tissue engineering. *Mol Aspects Med* 2002; 23(6): 463–483.
3. Rouwkema J, Rivron NC and van Blitterswijk CA. Vascularization in tissue engineering. *Trends Biotechnol* 2008; 26(8): 434–441.
4. Laschke MW, Harder Y, Amon M, et al. Angiogenesis in tissue engineering: breathing life into constructed tissue substitutes. *Tissue Eng* 2006; 12(8): 2093–2104.
5. Rophael JA, Craft RO, Palmer JA, et al. Angiogenic growth factor synergism in a murine tissue engineering model of angiogenesis and adipogenesis. *Am J Pathol* 2007; 171(6): 2048–2057.
6. Arkudas A, Tjiawi J, Bleiziffer O, et al. Fibrin gel-immobilized VEGF and bFGF efficiently stimulate angiogenesis in the AV loop model. *Mol Med* 2007; 13(9–10): 480–487.
7. Chen RR, Silva EA, Yuen WW, et al. Spatio-temporal VEGF and PDGF delivery patterns blood vessel formation and maturation. *Pharm Res* 2007; 24(2): 258–264.
8. Arkudas A, Pryymachuk G, Hoereth T, et al. Dose-finding study of fibrin gel-immobilized vascular endothelial growth factor 165 and basic fibroblast growth factor in the arteriovenous loop rat model. *Tissue Eng Part A* 2009; 15(9): 2501–2511.
9. Tanaka Y, Sung KC, Fumimoto M, et al. Prefabricated engineered skin flap using an arteriovenous vascular bundle as a vascular carrier in rabbits. *Plast Reconstr Surg* 2006; 117(6): 1860–1875.
10. Arkudas A, Tjiawi J, Saumweber A, et al. Evaluation of blood vessel ingrowth in fibrin gel subject to type and concentration of growth factors. *J Cell Mol Med* 2009; 13(9A): 2864–2874.
11. Tanaka Y, Tsutsumi A, Crowe DM, et al. Generation of an autologous tissue (matrix) flap by combining an arteriovenous shunt loop with artificial skin in rats: preliminary report. *Br J Plast Surg* 2000; 53(1): 51–57.
12. Hofer SO, Knight KM, Cooper-White JJ, et al. Increasing the volume of vascularized tissue formation in engineered constructs: an experimental study in rats. *Plast Reconstr Surg* 2003; 111(3): 1186–1192; discussion 1193–1194.
13. Lokmic Z, Stillaert F, Morrison WA, et al. An arteriovenous loop in a protected space generates a permanent, highly vascular, tissue-engineered construct. *FASEB J* 2007; 21(2): 511–522.
14. Manasseri B, Cuccia G, Moimas S, et al. Microsurgical arterovenous loops and biological templates: a novel in vivo chamber for tissue engineering. *Microsurgery* 2007; 27(7): 623–629.
15. Arsic N, Zacchigna S, Zentilin L, et al. Vascular endothelial growth factor stimulates skeletal muscle regeneration in vivo. *Mol Ther* 2004; 10(5): 844–854.
16. Arsic N, Zentilin L, Zacchigna S, et al. Induction of functional neovascularization by combined VEGF and angiopoietin-1 gene transfer using AAV vectors. *Mol Ther* 2003; 7(4): 450–459.

17. Ferrarini M, Arsic N, Recchia FA, et al. Adeno-associated virus-mediated transduction of VEGF165 improves cardiac tissue viability and functional recovery after permanent coronary occlusion in conscious dogs. *Circ Res* 2006; 98(7): 954–961.
18. Murphy SL and High KA. Gene therapy for haemophilia. *Br J Haematol* 2008; 140(5): 479–487.
19. Hasbrouck NC and High KA. AAV-mediated gene transfer for the treatment of hemophilia B: problems and prospects. *Gene Ther* 2008; 15(11): 870–875.
20. Zentilin L, Tafuro S, Zacchigna S, et al. Bone marrow mononuclear cells are recruited to the sites of VEGF-induced neovascularization but are not incorporated into the newly formed vessels. *Blood* 2006; 107(9): 3546–3554.
21. Zacchigna S, Pattarini L, Zentilin L, et al. Bone marrow cells recruited through the neuropilin-1 receptor promote arterial formation at the sites of adult neoangiogenesis in mice. *J Clin Invest* 2008; 118(6): 2062–2075.
22. Lovric J, Mano M, Zentilin L, et al. Terminal differentiation of cardiac and skeletal myocytes induces permissivity to AAV transduction by relieving inhibition imposed by DNA damage response proteins. *Mol Ther* 2012; 20(11): 2087–2097.
23. Zacchigna S, Tasciotti E, Kusmic C, et al. In vivo imaging shows abnormal function of vascular endothelial growth factor-induced vasculature. *Hum Gene Ther* 2007; 18(6): 515–524.
24. Rabinowitz JE, Rolling F, Li C, et al. Cross-packaging of a single adeno-associated virus (AAV) type 2 vector genome into multiple AAV serotypes enables transduction with broad specificity. *J Virol* 2002; 76(2): 791–801.
25. Wu Z, Asokan A and Samulski RJ. Adeno-associated virus serotypes: vector toolkit for human gene therapy. *Mol Ther* 2006; 14(3): 316–327.
26. Tafuro S, Ayuso E, Zacchigna S, et al. Inducible adeno-associated virus vectors promote functional angiogenesis in adult organisms via regulated vascular endothelial growth factor expression. *Cardiovasc Res* 2009; 83(4): 663–671.
27. Levy AP, Levy NS, Wegner S, et al. Transcriptional regulation of the rat vascular endothelial growth factor gene by hypoxia. *J Biol Chem* 1995; 270(22): 13333–13340.
28. Forsythe JA, Jiang BH, Iyer NV, et al. Activation of vascular endothelial growth factor gene transcription by hypoxia-inducible factor 1. *Mol Cell Biol* 1996; 16(9): 4604–4613.
29. Shweiki D, Itin A, Soffer D, et al. Vascular endothelial growth factor induced by hypoxia may mediate hypoxia-initiated angiogenesis. *Nature* 1992; 359(6398): 843–845.